applied sciences

MDPI

Article

The Magic Cocktail: Ampicillin and Biosynthesized Gold Nanoparticles Synergism against *Staphylococcus aureus*

Marco Oliveira [1,2,3], Silvia Soares [1,4,5], Sara Sá [1,4,5], Álvaro Gestoso [1,4], Miguel Correa-Duarte [6,7], Pilar Baylina [1,4,8], Rúben Fernandes [1,4,9,*] and Carla F. Pereira [3,*]

1 FP-BHS—Biomedical and Health Sciences Research Unit, FP-I3ID—Instituto de Investigação, Inovação e Desenvolvimento, FFP—Fundação Fernando Pessoa, 4420-096 Porto, Portugal; moliveirall97@gmail.com (M.O.); silvia_27_01@hotmail.com (S.S.); saravsa@ufp.edu.pt (S.S.); agestoso@ufp.edu.pt (Á.G.); pilarbaylina@ess.ipp.pt (P.B.)
2 CTBIO—Polytechnic, Institute of Porto, 4420-096 Porto, Portugal
3 CBQF—Centro de Biotecnologia e Química Fina—Laboratório Associado, Escola Superior de Biotecnologia, Universidade Católica Portuguesa, Rua Diogo Botelho 1327, 4169-005 Porto, Portugal
4 HE-FP, Hospital Fernando Pessoa, CECLIN—Center of Clinical Studies, 4420-096 Gondomar, Portugal
5 Faculty of Medicine, University of Porto, 4420-319 Porto, Portugal
6 CINBIO—Center for Research in Nanomaterials and Biomedicine, University of Vigo, 36310 Vigo, Spain; macorrea@uvigo.es
7 Faculty of Chemistry, Department of Physical Chemistry, University of Vigo, 36310 Vigo, Spain
8 School of Health of the Polytechnic, Institute of Porto, 4420-072 Porto, Portugal
9 Faculty of Health Sciences, Fernando Pessoa University, 420-150 Porto, Portugal
* Correspondence: ruben.fernandes@ufp.edu.pt (R.F.); cpfpereira@ucp.pt (C.F.P.)

Abstract: Gold nanoparticles (AuNPs) have garnered attention as a potential alternative to conventional antibiotics due to their innovative antibacterial properties. This study demonstrates the successful production of biosynthetic gold nanoparticles (bAuNPs) using *Pseudomonas aeruginosa* (*P. aeruginosa*) as spherical nanostructures at 58 °C for 24 h, under alkaline pH (9.0). The successful synthesis of bAuNPs was confirmed through UV-Vis spectroscopy, exhibiting a characteristic peak within the 500–600 nm wavelength range, and the evaluation of the main functional groups and morphology were stressed by Fourier Transform Infrared Spectroscopy (FT-IR) and Transmission Electron Microscopy (TEM), respectively. Subsequently, the synthesized bAuNPs were combined with low concentrations of ampicillin and evaluated against Methicillin-Susceptible *Staphylococcus aureus* (MSSA) and Methicillin-Resistant *Staphylococcus aureus* (MRSA) through the classical serial dilution method. This innovative approach holds the potential to address the escalating issue of antibiotic resistance, providing a viable and sustainable solution.

Keywords: antibiotic resistance; biosynthetic gold nanoparticles; ampicillin; synergism

Citation: Oliveira, M.; Soares, S.; Sá, S.; Gestoso, Á.; Correa-Duarte, M.; Baylina, P.; Fernandes, R.; Pereira, C.F. The Magic Cocktail: Ampicillin and Biosynthesized Gold Nanoparticles Synergism against *Staphylococcus aureus*. *Appl. Sci.* **2023**, *13*, 10934. https://doi.org/10.3390/app131910934

Academic Editor: Tatsuya Unno

Received: 31 August 2023
Revised: 26 September 2023
Accepted: 29 September 2023
Published: 3 October 2023

1. Introduction

Antibiotic usage has contributed to the emergence of antibiotic resistance, diminishing the bactericidal efficacy of antibiotics at previously effective doses. This phenomenon poses a significant threat to human life and health, as multidrug-resistant bacteria (MDR) have re-emerged, causing severe and incurable diseases [1]. In response to this challenge, researchers have turned to inorganic nanoparticles (NPs), such as silver nanoparticles (AgNPs), copper nanoparticles (CuNPs), and zinc nanoparticles (ZnONPs), as potential antibacterial agents. These NPs possess strong antibacterial properties and are less prone to the development of antibiotic resistance [2–4].

Various facets of nanomaterial-mediated antibacterial treatments are explored in available review articles. Notably, Mba and Nweze [5] extensively examine the challenges, opportunities, and advancements in nanomaterial-based antibacterial therapy against

MDR strains. Their insights emphasize the pressing need for innovative technologies in antibacterial treatments.

Furthermore, Gupta et al. [6] provides a tutorial review that elucidates the diverse con-tributions of nanomaterials to different treatment modalities against MDR bacteria. In a separate vein, Miller et al. [7] delve into inorganic NPs drug delivery capabilities, in-vestigating their release mechanisms within infected cells and elucidating techniques to enhance drug loading capacities through surface functionalization.

Concurrently, multiple research groups emphasize the importance of dynamic therapies reliant on reactive oxygen species (ROS) for eradicating bacteria. For instance, Ray et al. [8] have reported on targeted bacterial detection and photothermal elimination. In a multifaceted therapeutic context, Huo et al. [9] have defined an enhanced photothermal conversion efficiency, while Han et al. [10] have reviewed near-infrared (NIR) light-based antibacterial treatments. Moreover, beyond their potential applications in the therapeutic field, researchers have explored the utilization of these nanomaterials as disinfection agents. In a study conducted by Najafpoor et al. [11], magnetic silver nanoparticles were investigated for their promise in both disinfection and wastewater treatment. These diverse strands of research collectively underscore the pivotal role of nanomaterials and innovative technologies in the continuous evolution of antibacterial treatment strategies.

The mechanisms underlying the antibacterial activity of gold nanoparticles (AuNPs) encompass several key aspects. Due to their nanoscale dimensions, AuNPs can breach the bacterial cell membrane, potentially causing membrane destabilization and the release of cellular components. Furthermore, when exposed to light or other stimuli, AuNPs can generate reactive oxygen species (ROS), including free radicals, which can inflict damage upon proteins, lipids, and nucleic acids within the bacterial cell. AuNPs also damage proteins by interfering with existing disulfide bridges or thiol groups in various molecular systems within the cells. Some AuNPs possess the capability to impede bacterial growth by interfering with DNA replication or crucial metabolic processes. Additionally, they disrupt bacterial cellular respiration by impacting the electron transport chain and reducing the production of ATP, the cell's primary energy source. These nanoparticles also have the capacity to induce DNA damage, resulting in genetic mutations and possible cell demise, as well as perturb gene expression, leading to disruptions in normal cellular processes. Depending on their surface coating, AuNPs may accumulate in specific bacterial cellular components, such as the cell wall, plasma membrane, or cytoplasm, causing localized harm. Furthermore, they can induce oxidative stress in bacterial cells, triggering the oxidation of vital biomolecules, and interact with bacterial proteins, leading to alterations in their structure and function. While the exact mechanisms of AuNPs' antibacterial activity are not fully understood, there is evidence to suggest that they disrupt DNA and proteins through the uptake of free gold ions, increase oxidative stress by generating ROS, and directly interact with cellular membranes, as illustrated in Figure 1 [12–14].

Another approach to combat high-spectrum antibiotic-resistant bacteria involves augmenting the antibacterial action of antibiotics through the use of other agents. Gold nanoparticles (AuNPs), known for their inherent non-cytotoxic nature [15,16], have shown promise in enhancing the bactericidal activity of antibiotics such as carbapenems [17], linezolid [18], and streptomycin [19]. Various synthesis methods can be employed to produce AuNPs [20]. The most commonly used conventional method is the Turkevitch method, which involves the reduction of chloroauric acid $HAuCl_4$ using citrate-containing water [20]. Physical methods, including radiation (microwave, gamma irradiation, or ultraviolet), can also generate AuNPs by creating heat and a reducing environment. Laser ablation, another physical method utilizing lasers emitting specific wavelengths, is frequently employed for AuNP synthesis [21]. However, the use of hazardous chemicals, high temperatures, and expensive equipment associated with these methods has raised concerns regarding their ecological impact and sustainability. As a result, biosynthesized nanoparticles (bAuNPs) have emerged as a disruptive alternative to conventional synthesis methods, offering a more sustainable and eco-friendly approach. In addition to their sustainability, bAuNPs

possess avant-garde properties such as biocompatibility, bioavailability, bioactivity, and bioabsorption, making them attractive substitutes for conventionally synthesized NPs in various applications [22].

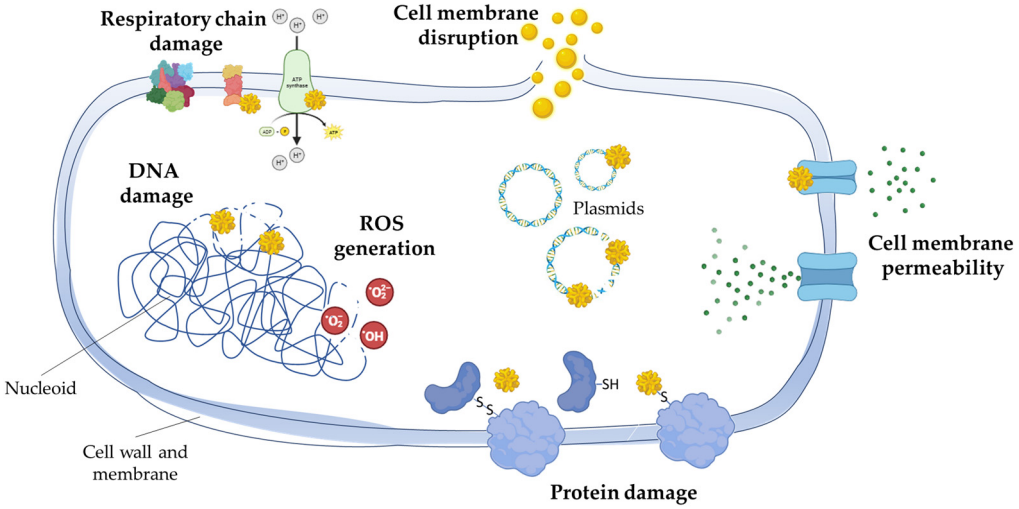

Figure 1. Mechanisms of action of gold nanoparticles on bacterial cells. Gold nanoparticles, due to their nanoscale size, can penetrate bacterial cell membranes, potentially destabilizing them and causing the leakage of cellular components. When exposed to light or other stimuli, these nanoparticles can generate reactive oxygen species (ROS), damaging proteins, lipids, and nucleic acids inside bacterial cells. In particular, gold nanoparticles damage proteins by interfering with existing disulfide bridges or thiol groups in the various biomolecular systems within the cells. Some gold nanoparticles inhibit bacterial growth by interfering with DNA replication or metabolic processes, while others disrupt cellular respiration, reducing ATP production. They can induce DNA damage, genetic mutations, and dysregulate gene expression. Depending on their coating, gold nanoparticles may accumulate in specific cellular components, causing localized damage and inducing oxidative stress. Additionally, they can interact with bacterial proteins, altering their structure and function.

Biosynthesized nanoparticles can be produced from different organisms, including plant tissues, actinomycetes, fungi, bacteria, algae, and others. Although some studies have described intracellular synthesis of bAuNPs using fungi, this approach is more complex and time-consuming compared to extracellular synthesis, which eliminates several recovery steps required for AuNP isolation [23]. Bacteria have become a widely studied microorganism for NP synthesis due to their simple culture conditions, ease of purification, and high synthesis yields [24]. The biosynthesis of nanoparticles involves the oxidation/reduction of metallic ions by biomolecules, such as proteins, enzymes, carbohydrates, and sugars, secreted by microorganisms [25]. Among the reductants found in nature, *Pseudomonas aeruginosa* extract has gained attention as an appealing option for the biosynthesis of gold nanoparticles. It has been shown to be more efficient than chemical synthesis methods, yielding AuNPs with promising antimicrobial activities [26]. Additionally, *P. aeruginosa* has the ability to produce a wide variety of compounds with bactericidal or bacteriostatic properties, including pyocyanin and other heterocyclic compounds like quinolines, phenylpyrroles, and phenazines, which could further enhance the antimicrobial potential of the resulting AuNPs [27].

Hence, employing *P. aeruginosa* extracts as a sustainable method to synthesize small-sized gold nanoparticles (AuNPs) capable of augmenting the antibacterial activity of antibiotics can prove to be an effective strategy in combating superbugs. The class of β-lactam antibiotics holds immense significance as it is present in more than 34 U.S. Food and Drug Administration (FDA)-approved medications, accounting for approximately half of all antibiotics [28]. However, the emergence of β-lactam resistance has significantly impacted empirical therapy [29]. To tackle this challenge, the present study utilized

P. aeruginosa extracts to generate biosynthetic small-sized AuNPs. These resulting AuNPs were combined with low concentrations of ampicillin (Amp) to create a cocktail, which was then tested against MSSA and MRSA.

The aim of this study was to introduce a biosynthetic approach for reducing $HAuCl_4$ salts into nanoparticles, thereby circumventing the use of toxic chemical substances that have significant environmental implications. Furthermore, the antibacterial potential of these biosynthesized nanoparticles was evaluated against both MRSA and MSSA. This study introduces a novel approach by harnessing AuNPs biosynthesized with *P. aeruginosa*, a bacterium with inherent antibacterial properties often underappreciated in this context. These AuNPs are combined with minimal ampicillin doses, offering a potential solution to address MRSA's resistance to β-lactam antibiotics. Additionally, the study pioneers the biosynthesis of these AuNPs under specific conditions (pH 9, 58 °C, 24 h), resulting in the production of small, spherical nanoparticles not previously documented in the literature.

2. Materials and Methods

2.1. Chemicals

Gold(III) chloride, $HAuCl_4$ (ACS reagent), was obtained from Sigma Aldrich, St. Louis, MO, USA, and used without further purification. All other reagents used in this study were of analytical grade.

2.2. Pseudomonas aeruginosa Strain and Maintenance

P. aeruginosa (ATCC 15692) was purchased and maintained by Laboratory of Medical and Industrial biotechnology (LaBMI), Porto Research, Technology & Innovation Center (PORTIC), Porto, Portugal. Bacteria were routinely cultured in Trypticase soy agar (TSA) plates where the fluorescent pigment pyoverdine typically produced by *P. aeruginosa* strains was observed.

2.3. bAuNPs Synthesis

P. aeruginosa was cultured at OD600 = 0.1 in 100 mL TSB and maintained at 150 rpm for 9 h at 37 °C. The supernatant was recovered by centrifugation at 4000 rpm. After, a $HAuCl_4$ solution (50 mM) was mixed with the cell free supernatant. The resulting solution was submitted to a pH manipulation using 0.1 M NaOH until reach pH (9.0). The synthesis was conducted at 58 °C for 24 h. Control solutions (without the addition of HAuCl4) were also run along with the experimental tubes and subjected to the same reaction conditions.

2.4. bAuNPs Characterization

2.4.1. Ultraviolet-Visible Spectroscopy (UV-Vis Spectroscopy)

To confirm the presence of AuNPs, the excitation spectra of the samples were measured by UV-Vis spectroscopy using the Multiskan SkyHigh spectrophotometer (Thermo Fisher Scientific, Waltham, MA, USA). The pellets of control and AuNPs solutions were resuspended in DEPC (diethyl pyrocarbonate)-treated water (Thermo Fisher Scientific, Waltham, MA, USA), mixed by vortexing, and the excitation spectra were recorded in a wavelength range of 300 to 700 nm. All measurements were done in a quartz cuvette (1 mm). Concentrations of gold ions that were reduced to AuNPs in the biosynthesis process were calculated following Scarabelli et al. [30] correlation, where, from the absorbance at 400 nm and for a 1 mm cuvette, an absorbance of 1.2 (OD_{400}) corresponds to [Au0] = 0.5 mM:

$$A_{400nm} = 1.2 \Leftrightarrow [Au^0] = 0.5\ mM \quad (1)$$

2.4.2. Transmission Electron Microscopy (TEM)

10 µL of each sample was mounted on carbon film-coated mesh nickel grids and left standing for 2 min. The excess liquid was removed with filter paper from all samples, and the grids were observed in a JEM 1400 TEM (JOEL Ltd., Tokyo, Japan) with an accelerating voltage of 80 kV. Images were digitally recorded using a CCD digital camera (Orious 1100W

Tokyo, Japan). After, images were analyzed using ImageJ version 1.54f API (U. S. National Institutes of Health, Bethesda, MD, USA) software to assess the mean particle size.

2.4.3. Attenuated Total Reflection Fourier-Transform Infrared Spectroscopy (ATR-FT-IR)

The ATR-FT-IR analyses were performed using the Frontier™ MIR/FIR spectrometer from PerkinElmer in a scanning range of 550–4000 cm^{-1} for 16 scans at a spectral resolution of 4 cm^{-1}. Prior to analysis all samples were lyophilized (Model Alpha 2–4 LSCplus—Christ, Osterode am Harz, Germany).

2.5. bAuNPs and Ampicillin Effect on Bacteria Growth

The influence of gold nanoparticles in the kinetics growth curve was tested on two strains of *S. aureus*. For the present study, it was used a methicillin-resistant *S. aureus* (MRSA, ATCC 43300) and a methicillin-susceptible *S. aureus* (MSSA, ATCC 25923). All strains were cultured in Muller-Hinton Broth (MHB) and adjusted to 0.1 (OD600).

The effect of bAuNPs and ampicillin in bacterial growth was first tested separately and using the serial dilution method. Final concentrations of bAuNPs ranging from 0.5 to 0.0001 mM and final concentrations of antibiotic ranging from 10 to 0.00001 mg/L were added to the cultures. Cultures were placed in 96 well plates adding 200 µL of the final solution in each well and maintaining at 37 °C for 24 h. Absorbances (OD600) were measured every 30 min using the Multiskan SkyHigh spectrophotometer (Thermo Fisher Scientific, Waltham, MA, USA) over a 24 h period. Control wells containing only medium, and bacteria were monitored in the same conditions throughout the experiment.

bAuNPs were tested again under the same conditions but adding only 0.1 mM of solution concentration in both bacteria. Ampicillin was tested at a concentration of 0.01 mg/L for MSSA and 0.1 mg/L for MRSA. Cultures were also done with the addition of a mixture of bAuNPs and ampicillin in the same concentrations. The growth was again monitored for 24 h using the spectrophotometer.

The area under the curve (AUC) was calculated using GraphPad prism 9.0.0 (GraphPad Software, Inc., San Diego, CA, USA), which was used as cumulative measure of the effect of the bAuNPs in the total growth of bacteria.

2.6. bAuNPs and Ampicillin Effect on Bacteria Viability

After 24 h growth, each culture was submitted to serial dilutions ranging from 1 to 10^{-8}. 10 ul of each solution was plated in MHA plates. After 12 h growth, the colony forming units (CFU) were counted under a magnifying glass. All cultures were grown at 37 °C for 24 h in triplicate and the colonies were counted in a magnifying glass. After, CFU/mL was calculated using the following equation:

$$\frac{\text{CFU}}{\text{mL}} = \frac{\text{N}^{\text{o}} \text{ of colonies}}{\text{Volume of culture plated (mL)}} \times \text{dilution} \quad (2)$$

where CFU/mL is the number of colony-forming units per milliliter; N° of colonies is the number of colonies on the culture plate; Volume of culture plated (mL) is the volume of the culture that was plated on the plate, measured in milliliters and dilution is the dilution factor used when plating the culture.

2.7. Statistics Analysis

All data was analyzed as the mean ± standard deviation (SD). All the assays were repeated in triplicate for statistical analysis. The statistical significance was determined using Student *t* test, 1-way analysis of variance analysis. Results were considered significant when * $p < 0.05$, ** $p < 0.01$, *** $p < 0.001$ and **** $p < 0.0001$. All analyses were performed in GraphPad prism version 9.0.0 (GraphPad Software, Inc., San Diego, CA, USA).

3. Results and Discussion

3.1. bAuNPs Characterization

3.1.1. UV-Vis and TEM

A few hours after adding chloroauric acid to the bacterial supernatant, the synthesis of nanoparticles was initially identified by the color change of the solutions to red (Figure 2a). The synthesis of bAuNPs was confirmed using UV-Vis spectroscopy, which revealed characteristic peaks in the wavelength range of 500–600 nm (Figure 2a). UV-Vis spectroscopy was employed to determine the concentration and aggregation of bAuNPs.

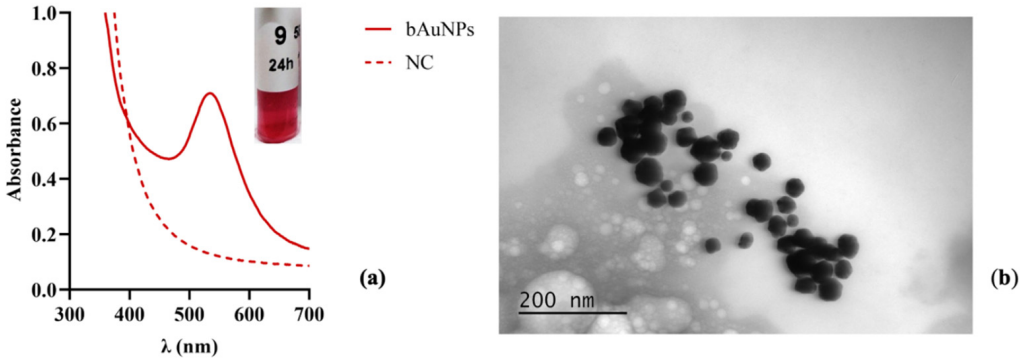

Figure 2. UV-vis spectrum and TEM photographs of the obtained bAuNPs at 58 °C under alkaline pH (9.0) for 24 h: (**a**) UV-Vis spectra and the colloidal solution obtained for bAuNPs synthesized. (**b**) TEM photographs (200 nm). Note: NC refers to the normal condition, which represents the basal medium only, while bAuNPs represents biosynthetic gold nanoparticles.

The morphological features, including shape and size, were determined using TEM. TEM analysis (Figure 2b) demonstrated that under alkaline pH (9.0) and at 58 °C for 24 h, the gold nanoparticles exhibited a spherical structure and reduced sizes (30.862 ± 13.48). The synthesis methodology of AuNPs follows two steps: (I) nucleation and (II) growth phase. Nucleation is the process in which a cluster, a particle from a new phase, is formed in a single-phase system. In the chemistry of AuNPs synthesis, these clusters are referred to as nuclei.

The critical radius of these clusters is related to the smallest size at which a particle can remain in solution without redissolving. During the growth stage, more material is deposited on the cluster, increasing its size and transforming it into a nanoparticle. This is caused by the spread of growing species as well as surface processes [31]. At a high pH, the OH^- ions present in the extract replace the Cl^- ions present in the $AuCl4^-$, preventing the possible subsequent growth of the nuclei due to repulsions between negatively charged ions of the cell extract and gold ions. This may explain why the bAuNPs synthesized at pH 9.0 maintain a small size and spherical shape [32].

3.1.2. ATR-FT-IR

The ATR-FT-IR spectrum (Figure 3) exhibits a strong and broad vibration band at 3267 cm^{-1}, which can be assigned to the stretching of the hydroxyl groups. Additionally, a weak vibration at 3076 cm^{-1}, characteristic of N-H stretching, and an absorption peak at approximately 2965 cm^{-1}, attributed to the C-H stretching vibration of alkanes, are observed. All ATR-FT-IR spectra also show vibrations at 1632 and 1579 cm^{-1}, which can be assigned to amides containing carbonyl groups (C=O), as well as absorption bands at 1453, 1399, and 1077 cm^{-1}, attributed to the C-O stretching vibrations of aromatic and aliphatic amines, respectively [33]. The presence of various compounds suggests the involvement of organic molecules in the bAuNPs synthesis process. The presence of amines, likely due to amino acid residues, indicates the coexistence of proteins from *P. aeruginosa* extract with bAuNPs. This finding leads to the hypothesis that these coexisting proteins could be one of the factors influencing the rate of internalization of bAuNPs in tumor and bacterial cells.

Consequently, there is a reduced probability of cells recognizing bAuNPs as foreign agents and instead internalizing them as a food supplement.

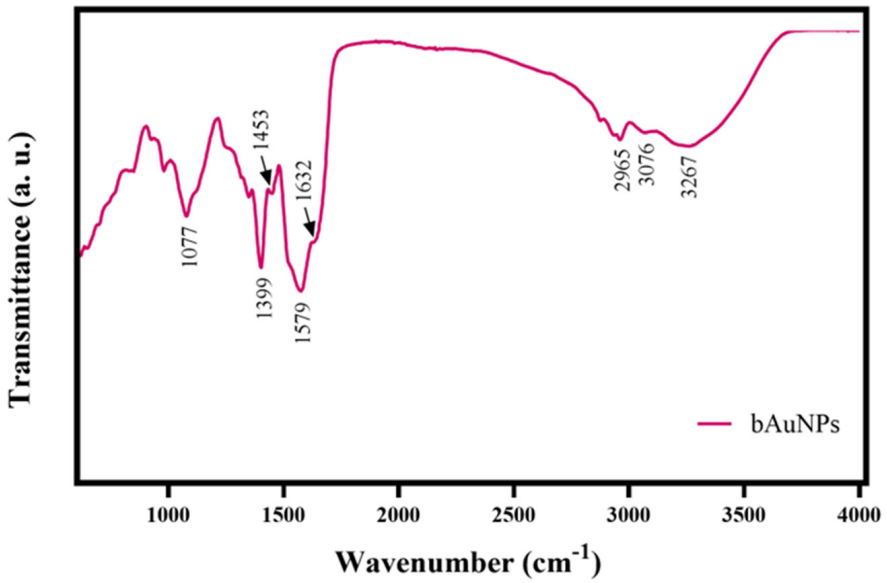

Figure 3. ATR-FT-IR spectrum of the bAuNPs synthesized at 58 °C under alkaline pH (9.0) for 24 h.

3.2. bAuNPs and Ampicillin Effect on Bacterial Growth and Viability

The data obtained from the preliminary screening analysis of the effect of bAuNPs on the growth of MSSA and MRSA, tested across a concentration range of 0.5 mM to 0.0001 mM, revealed a statistically significant reduction in growth when bAuNPs were applied at a concentration of 0.1 mM. The growth inhibition percentages were 59% for MSSA (Figure 4c) and 57% for MRSA (Figure 4d), respectively ($p < 0.01$).

However, no dose-dependent effect was observed with increasing concentration of bAuNPs. These findings contradict the results reported by Ahmad et al. and Folorunso et al. [34,35], but they support the notion that the effect of bAuNPs is not linearly correlated with concentration. This underscores the importance of selecting an optimal concentration. Based on this, a concentration of 0.1 mM of bAuNPs was chosen for the subsequent assays.

In contrast, the results obtained for the effect of ampicillin on the growth of MSSA and MRSA exhibited an increase with increasing dose. The effect of this antibiotic showed statistical significance in MSSA (Figure 4a) at concentrations of 10, 1, and 0.1 mg/L, resulting in decreases of 66% ($p < 0.0001$), 28% ($p < 0.05$), and 22% ($p < 0.05$), respectively. In MRSA (Figure 4b), decrease of 17% and 14% ($p < 0.05$) were observed at concentrations of 10 and 1 mg/L, respectively. As the effect of the antibiotic showed a consistent pattern with increasing dose, the chosen concentrations for the subsequent assays were the lowest concentrations immediately following those that demonstrated a statistically significant bacterial growth decrease. Therefore, the chosen concentration for MSSA was 0.01 mg/L (20% growth decrease) and for MRSA, it was 0.1 mg/L (12% growth decrease).

Ampicillin and bAuNPs were retested against MSSA and MRSA, and the results indicate a synergistic effect when the antibiotic is combined with bAuNPs, leading to a significant decrease in bacterial growth. The application of ampicillin resulted in a growth decline of 20% for MSSA (Figure 5a,c) and 13% for MRSA (Figure 5b,d). When bAuNPs were used alone, they exhibited a growth decrease of 60% for MSSA (Figure 4a,c) and 58% for MRSA (Figure 5b,d) ($p < 0.01$). However, when ampicillin was applied in combination with bAuNPs, a synergistic effect was observed, resulting in a remarkable bacterial growth decrease of 84% and 78% ($p < 0.001$) for MSSA (Figure 4a,c) and MRSA (Figure 5b,d), respectively.

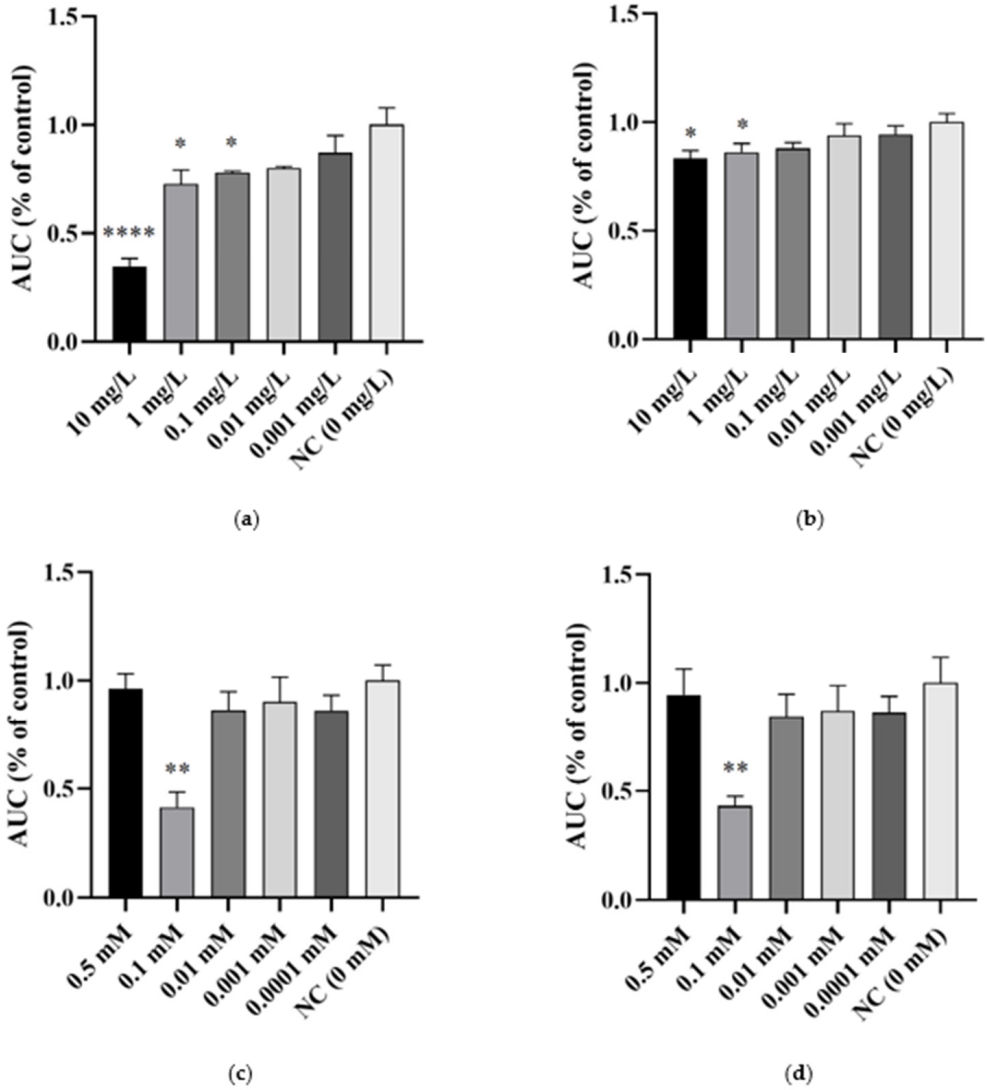

Figure 4. The effect of different concentrations of ampicillin and bAuNPs on bacterial growth expressed as the percentage of control AUC (area under the curve): (**a**) Effect of ampicillin on MSSA growth; (**b**) Effect of ampicillin on MRSA growth; (**c**) Effect of bAuNPs on MSSA growth; (**d**) Effect of bAuNPs on MRSA growth; AUC—area under the curve. NC—normal condition, i.e., basal medium only. * $p < 0.05$, ** $p < 0.01$, **** $p < 0.0001$.

To assess the impact on cell viability, ampicillin and bAuNPs were further tested on MSSA and MRSA under the same experimental conditions, and the number of colony-forming units (CFUs) was determined. The results, presented in Table 1 and Figure 6, indicate that both agents exhibited inhibitory effects on the cell viability of both bacterial strains. Treatment with ampicillin alone resulted in a 13% reduction in viability for MSSA (Figure 6a) and a 12% reduction for MRSA (Figure 6b). Similarly, bAuNPs demonstrated their efficacy by reducing viability by 49% in MSSA (Figure 6a) and 40% in MRSA (Figure 6b) ($p < 0.01$). Remarkably, the synergistic effect persisted when ampicillin was combined with bAuNPs, leading to a substantial reduction in cell viability of 74% ($p < 0.001$) for MSSA (Figure 5a) and 66% ($p < 0.01$) for MRSA (Figure 6b).

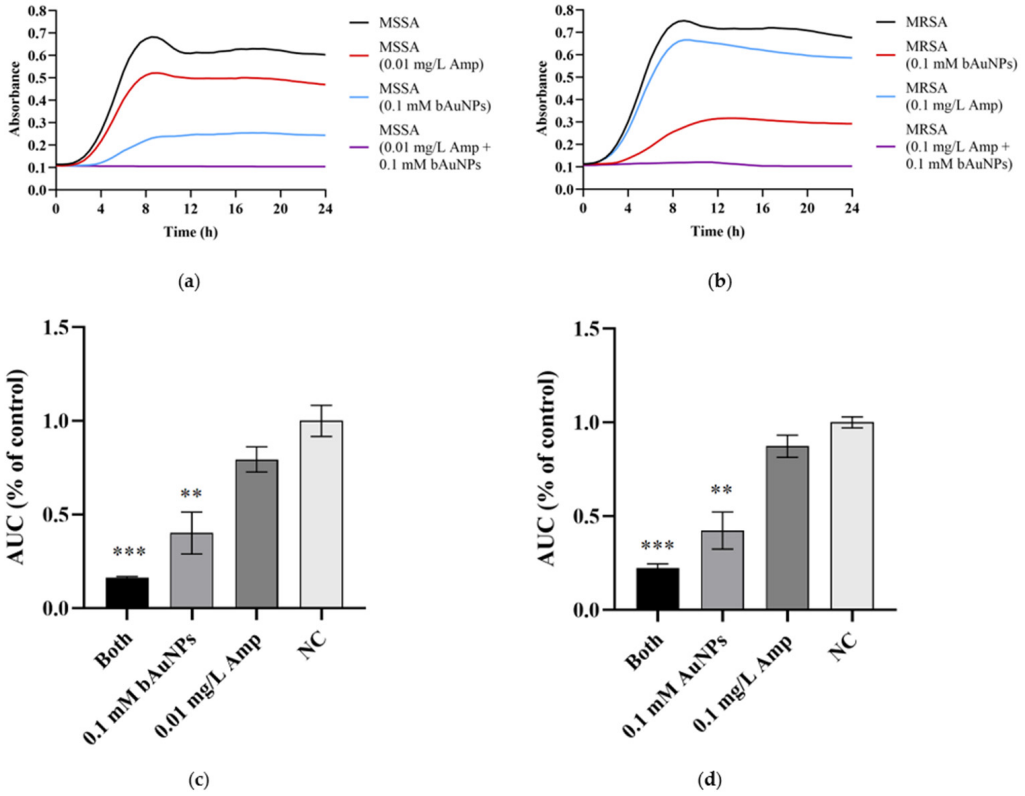

Figure 5. Effect of specific concentrations of ampicillin and bAuNPs on bacterial growth: (**a**) MSSA growth curves; (**b**) MRSA growth curves; (**c**) effect of ampicillin, bAuNPs and both (0.01 mg/L Amp and 0.1 mM bAuNPs) on MSSA growth expressed in AUC as percentage of control; (**d**) effect of ampicillin, bAuNPs and both (0.1 mg/L Amp and 0.1 mM bAuNPs) on MRSA growth expressed in AUC as percentage of control. AUC—area under the curve; NC—normal condition, i.e., basal medium only; Amp—ampicillin; bAuNPs—biosynthetic gold nanoparticles; Both—a mixture of bAuNP and ampicillin; MSSA—Methicillin-susceptible *S. aureus*; MRSA—Methicillin-resistant *S. aureus*; CFU—colony-forming units. ** $p < 0.01$, *** $p < 0.001$.

Table 1. Effect of ampicillin and bAuNPs in MSSA and MRSA viability.

Agent	Growth Condition	CFU/mL
MSSA	NC	3.93×10^8
	0.001 mg/L Amp	3.40×10^8
	0.1 mM bAuNPs	2.00×10^8
	Both	1.05×10^8
MRSA	NC	4.40×10^8
	0.001 mg/L Amp	3.85×10^8
	0.1 mM bAuNPs	2.63×10^8
	Both	1.48×10^8

Legend: NC—normal condition, i.e., basal medium only; Amp—ampicillin; bAuNPs—biosynthetic gold nanoparticles; MSSA—Methicillin-susceptible *S. aureus*; MRSA—Methicillin-resistant *S. aureus*; CFU—colony-forming units.

Gold nanoparticles (AuNPs) have garnered significant interest as potential carriers for antibiotic drugs. Several studies have explored the use of AuNPs to deliver antibiotics, and these investigations support the notion that the effectiveness of antibiotics remains unchanged when attached to AuNPs [36–39]. The conjugation of antibiotics with AuNPs offers the potential for enhanced therapeutic outcomes and improved drug delivery to target bacterial infections.

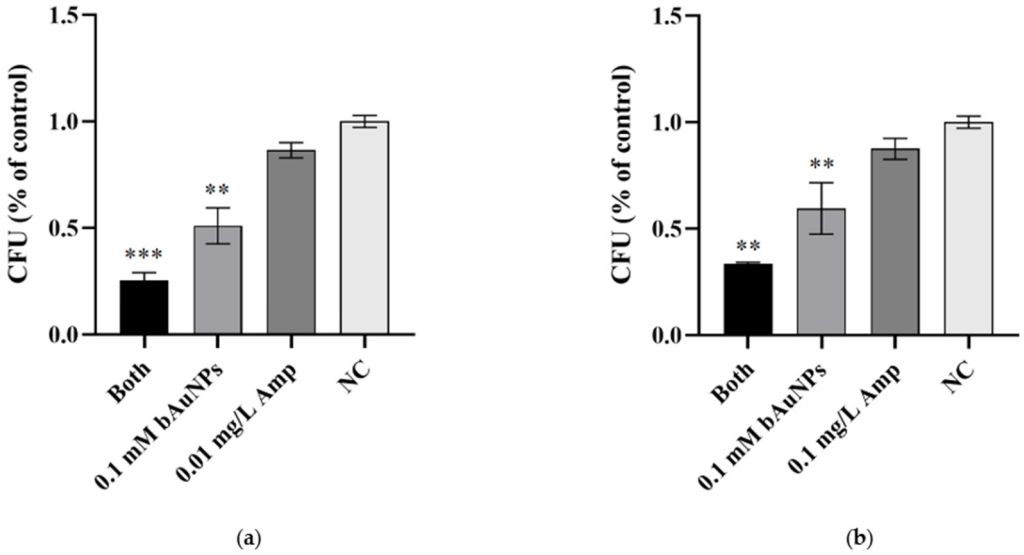

Figure 6. Effect of ampicillin and bAuNPs on bacterial viability: (**a**) Viability of MSSA expressed in CFU/mL as a percentage of control after treatment with ampicillin, bAuNPs, and both (0.01 mg/L Amp and 0.1 mM bAuNPs); (**b**) Viability of MRSA expressed in CFU/mL as a percentage of control after treatment with ampicillin, bAuNPs, and both (0.1 mg/L Amp and 0.1 mM bAuNPs). NC—Normal condition, i.e., basal medium only; Amp—Ampicillin; bAuNPs—Biosynthetic gold nanoparticles; Both—A mixture of bAuNPs and ampicillin; CFU—Colony-forming units. ** $p < 0.01$, *** $p < 0.001$.

In previous studies, the quantitative evaluation of the efficacy of antibiotic-AuNP conjugates against bacteria remained uncertain. Most reports determined the Minimum Inhibitory Concentrations (MICs) of the agents by measuring the decrease in optical density or by utilizing aggregated AuNPs [40]. However, in the present research, colony forming unit counting was employed as a quantitative method to assess the individual and combined effects of each agent on bacterial viability. This approach provides a more accurate and reliable measure of the impact on bacterial growth and survival.

The observed synergistic effect of ampicillin in combination with bAuNPs suggests that bAuNPs play a role in enhancing the penetration of ampicillin into the bacterial cell wall. This enhanced penetration leads to increased interactions between ampicillin and bacteria, ultimately improving the efficacy of the antibiotic. It is important to note that the resistance of *S. aureus* to antibiotics, such as ampicillin, is primarily attributed to the production of the penicillin-binding protein 2a (PBP-2a). This protein exhibits lower affinity for β-lactam antibiotics, thereby reducing the effectiveness of these drugs [41]. Consequently, the results obtained in this study imply that bAuNPs might enhance the affinity of bacteria to ampicillin, potentially overcoming the resistance mechanism mediated by PBP-2a. This enhanced affinity could disrupt the bacterial cell wall, further contributing to the reduction in bacterial growth and viability.

Nevertheless, the exact mechanism of action of bAuNPs on bacteria remains incompletely understood and necessitates further investigation. Future research efforts can focus on elucidating the precise molecular interactions between bAuNPs and bacteria, as well as the impact of these interactions on the integrity of the bacterial cell wall. Such studies will contribute to a more comprehensive understanding of the potential applications of bAuNPs in combating antibiotic-resistant bacteria.

4. Conclusions

In conclusion, our study demonstrated that biosynthetic AuNPs using biomass extracts of *P. aeruginosa* at 58 °C and alkaline pH (9.0) resulted in the formation of small spherical nanoparticles with reduced size, as confirmed by UV-Vis and TEM analyses. The preliminary antibacterial screening revealed a statistically significant reduction in

the growth of MSSA and MRSA when exposed to bAuNPs. Moreover, the combination of ampicillin and bAuNPs exhibited a synergistic effect, significantly reducing bacterial growth and viability, thereby enhancing the individual effects of both agents.

Our findings suggest that bAuNPs enhance the penetration of ampicillin into the bacterial cell wall, increasing its efficacy. Additionally, it is possible that bAuNPs enhance the affinity of bacteria to the antibiotic, leading to the disruption of the cell wall. This strategy holds promise for combating antibiotic-resistant bacteria.

Furthermore, the use of *P. aeruginosa* extract as a green reduction system for bAuNP synthesis offers a more sustainable and environmentally friendly alternative to traditional synthesis methods. The valorization of bAuNPs stands as a pivotal achievement of this study. Derived from diverse organisms including plants, fungi, and bacteria, bAuNPs are extracellularly synthesized for efficiency, circumventing intricate intracellular processes and recovery steps. Bacteria, especially *P. aeruginosa*, excel in nanoparticle synthesis due to simple culture conditions and the reduction of metallic ions using biomolecules. Also, the biomass extracts of *P. aeruginosa* yields bAuNPs with potent antimicrobial potential, boosted by antibacterial compounds like pyocyanin. Adopting *P. aeruginosa* extracts for bAuNP synthesis transforms antibacterial strategies, augmenting both their direct activity and antibiotic efficacy. This approach gains significance against antibiotic-resistant superbugs. The fusion of biosynthetic AuNPs with low ampicillin concentrations presents a promising synergy, impactful against Methicillin-Susceptible and Methicillin-Resistant *S. aureus*, showcasing a transformative path for combating resistance.

Overall, the utilization of biosynthetic AuNPs as carriers for antibiotics, such as ampicillin, holds significant promise in improving antibacterial therapies. The synergistic effects observed in this study highlight the potential of bAuNPs to enhance the efficacy of antibiotics and combat antibiotic resistance. Further advancements in this field could lead to the development of novel therapeutic strategies to address the challenges posed by multidrug-resistant bacteria and contribute to the fight against infectious diseases.

In the face of the escalating global health concern posed by antibiotic-resistant bacteria, the strategy employed in this study presents a formidable approach. The fusion of biosynthetic AuNPs with established antibiotics not only showcases the power of interdisciplinary collaboration but also promises to reshape antibacterial therapeutic paradigms.

Author Contributions: Conceptualization, M.O., S.S. (Sílvia Soares) and R.F.; methodology, M.O., M.C.-D. and C.F.P.; software, M.O. and C.F.P.; validation, M.O., C.F.P. and R.F.; formal analysis, M.O., C.F.P. and R.F.; investigation, M.O., S.S. (Sílvia Soares), S.S. (Sara Sá), Á.G., M.C.-D., P.B., R.F. and C.F.P.; resources, P.B. and R.F.; data curation, M.O., C.F.P. and R.F.; writing—original draft preparation, M.O. and C.F.P.; writing—review and editing, M.C.-D., C.F.P. and R.F.; visualization, M.O.; supervision, R.F.; project administration, R.F.; funding acquisition, P.B. and R.F. All authors have read and agreed to the published version of the manuscript.

Funding: R.F. and P.B. acknowledges on the behalf of the authors the support of FCT (Strategic Project Reference: UID/BIM/04293/2013. R.F. and P.B. ware also supported by FEDER/02/SAICT/2020/072560. M.O. was funded by LaBMI, grant number PORTIC/IPP4COVID/BI/2021/01.

Institutional Review Board Statement: Not applicable.

Informed Consent Statement: Not applicable.

Data Availability Statement: Data will be available upon request to the corresponding authors.

Conflicts of Interest: The authors declare no conflict of interest.

References

1. Molina-Santiago, C.; de Vicente, A.; Romero, D. The race for antimicrobials in the multidrug resistance era. *Microb. Biotechnol.* **2018**, *11*, 976–978. [CrossRef] [PubMed]
2. Li, M.; Huang, L.; Wang, X.; Song, Z.; Zhao, W.; Wang, Y.; Liu, J. Direct generation of Ag nanoclusters on reduced graphene oxide nanosheets for efficient catalysis, antibacteria and photothermal anticancer applications. *J. Colloid Interface Sci.* **2018**, *529*, 444–451. [CrossRef] [PubMed]

3. Katwal, R.; Kaur, H.; Sharma, G.; Naushad, M.; Pathania, D. Electrochemical synthesized copper oxide nanoparticles for enhanced photocatalytic and antimicrobial activity. *J. Ind. Eng. Chem.* **2015**, *31*, 173–184. [CrossRef]
4. Sun, Q.; Li, J.; Le, T. Zinc Oxide Nanoparticle as a Novel Class of Antifungal Agents: Current Advances and Future Perspectives. *J. Agric. Food Chem.* **2018**, *66*, 11209–11220. [CrossRef]
5. Mba, I.E.; Nweze, E.I. Nanoparticles as therapeutic options for treating multidrug-resistant bacteria: Research progress, challenges, and prospects. *World J. Microbiol. Biotechnol.* **2021**, *37*, 1–30. [CrossRef]
6. Gupta, A.; Mumtaz, S.; Li, C.H.; Hussain, I.; Rotello, V.M. Combatting antibiotic-resistant bacteria using nanomaterials. *Chem. Soc. Rev.* **2019**, *48*, 415–427. [CrossRef]
7. Miller, K.P.; Wang, L.; Benicewicz, B.C.; Decho, A.W. Inorganic nanoparticles engineered to attack bacteria. *Chem. Soc. Rev.* **2015**, *44*, 7787–7807. [CrossRef]
8. Yougbaré, S.; Mutalik, C.; Krisnawati, D.I.; Kristanto, H.; Jazidie, A.; Nuh, M.; Cheng, T.M.; Kuo, T.R. Nanomaterials for the Photothermal Killing of Bacteria. *Nanomaterials* **2020**, *10*, 1123. [CrossRef]
9. Huo, J.; Jia, Q.; Huang, H.; Zhang, J.; Li, P.; Dong, X.; Huang, W. Emerging photothermal-derived multimodal synergistic therapy in combating bacterial infections. *Chem. Soc. Rev.* **2021**, *50*, 8762–8789. [CrossRef]
10. Han, Q.; Lau, J.W.; Do, T.C.; Zhang, Z.; Xing, B. Near-Infrared Light Brightens Bacterial Disinfection: Recent Progress and Perspectives. *ACS Appl. Bio Mater.* **2020**, *4*, 3937–3961. [CrossRef]
11. Najafpoor, A.; Norouzian-Ostad, R.; Alidadi, H.; Rohani-Bastami, T.; Davoudi, M.; Barjasteh-Askari, F.; Zanganeh, J. Effect of magnetic nanoparticles and silver-loaded magnetic nanoparticles on advanced wastewater treatment and disinfection. *J. Mol. Liq.* **2020**, *303*, 112640. [CrossRef]
12. Abdel-Raouf, N.; Al-Enazi, N.M.; Ibraheem, B.M. Green biosynthesis of gold nanoparticles using *Galaxaura elongata* and characterization of their antibacterial activity. *Arab. J. Chem.* **2017**, *10* (Suppl. S2), S3029–S3039. [CrossRef]
13. Timoszyk, A.; Grochowalska, R. Mechanism and Antibacterial Activity of Gold Nanoparticles (AuNPs) Functionalized with Natural Compounds from Plants. *Pharmaceutics* **2022**, *14*, 2599. [CrossRef] [PubMed]
14. Correa, M.G.; Martínez, F.B.; Vidal, C.P.; Streitt, C.; Escrig, J.; de Dicastillo, C.L. Antimicrobial metal-based nanoparticles: A review on their synthesis, types and antimicrobial action. *Beilstein J. Nanotechnol.* **2020**, *11*, 1450–1469. [CrossRef] [PubMed]
15. Zhao, Y.; Chen, Z.; Chen, Y.; Xu, J.; Li, J.; Jiang, X. Synergy of non-antibiotic drugs and pyrimidinethiol on gold nanoparticles against superbugs. *J. Am. Chem. Soc.* **2013**, *135*, 12940–12943. [CrossRef] [PubMed]
16. Cui, Y.; Zhao, Y.; Tian, Y.; Zhang, W.; Lü, X.; Jiang, X. The molecular mechanism of action of bactericidal gold nanoparticles on *Escherichia coli*. *Biomaterials* **2012**, *33*, 2327–2333. [CrossRef]
17. Park, M.V.D.Z.; Neigh, A.M.; Vermeulen, J.P.; de la Fonteyne, L.J.J.; Verharen, H.W.; Briedé, J.J.; van Loveren, H.; Jong, W.H. The effect of particle size on the cytotoxicity, inflammation, developmental toxicity and genotoxicity of silver nanoparticles. *Biomaterials* **2011**, *32*, 9810–9817. [CrossRef]
18. Bagga, B.; Buckingham, S.; Arnold, S.; Nesbitt, A.; Guimera, D.; Lee, K. Increasing Linezolid-resistant Enterococcus in a Children's Hospital. *Pediatr. Infect. Dis. J.* **2018**, *37*, 242–244. [CrossRef]
19. Mazdeh, S.; Motamedi, H.; Khiavi, A.; Mehrabi, M. Gold Nanoparticle Biosynthesis by *E. coli* and Conjugation with Streptomycin and Evaluation of its Antibacterial Effect. *Curr. Nanosci.* **2014**, *10*, 553–561. [CrossRef]
20. Ye, Y.; Lv, M.; Zhang, X.; Zhang, Y. Colorimetric determination of copper(ii) ions using gold nanoparticles as a probe. *RSC Adv.* **2015**, *5*, 102311–102317. [CrossRef]
21. Liu, X.Y.; Wang, J.Q.; Ashby, C.R.; Zeng, L.; Fan, Y.F.; Chen, Z.S. Gold nanoparticles: Synthesis, physiochemical properties and therapeutic applications in cancer. *Drug Discov. Today* **2021**, *26*, 1284–1292. [CrossRef]
22. Salem, S.S.; Fouda, A. Green Synthesis of Metallic Nanoparticles and Their Prospective Biotechnological Applications: An Overview. *Biol. Trace Elem. Res.* **2021**, *199*, 344–370. [CrossRef] [PubMed]
23. Ahmed, S.; Annu Ikram, S.; Yudha, S. Biosynthesis of gold nanoparticles: A green approach. *J. Photochem. Photobiol. B* **2016**, *161*, 141–153. [CrossRef] [PubMed]
24. Srinath, B.S.; Namratha, K.; Byrappa, K. Eco-Friendly Synthesis of Gold Nanoparticles by *Bacillus subtilis* and Their Environmental Applications. *Adv. Sci. Lett.* **2018**, *24*, 5942–5946. [CrossRef]
25. Iqtedar, M.; Aslam, M.; Akhyar, M.; Shehzaad, A.; Abdullah, R.; Kaleem, A. Extracellular biosynthesis, characterization, optimization of silver nanoparticles (AgNPs) using *Bacillus mojavensis* BTCB15 and its antimicrobial activity against multidrug resistant pathogens. *Prep. Biochem. Biotechnol.* **2019**, *49*, 136–142. [CrossRef]
26. Timoszyk, A.; Niedbach, J.; Ślizewska, P.; Mirończyk, A.; Kozioł, J.J. Eco-Friendly and Temperature Dependent Biosynthesis of Gold Nanoparticles Using the Bacterium *Pseudomonas aeruginosa*: Characterization and Antibacterial Activity. *J. Nano Res.* **2017**, *48*, 114–124. [CrossRef]
27. Onbasli, D.; Aslim, B. Determination of antimicrobial activity and production of some metabolites by *Pseudomonas aeruginosa* B1 and B2 in sugar beet molasses. *Afr. J. Biotechnol.* **2010**, *7*, 4614–4619.
28. King, D.T.; Sobhanifar, S.; Strynadka, N.C.J. The mechanisms of resistance to β-lactam antibiotics. *Handb. Antimicrob. Resist.* **2017**, *23*, 177–201.
29. Rossolini, G.M.; Mantengoli, E. Antimicrobial resistance in Europe and its potential impact on empirical therapy. *Clin. Microbiol. Infect.* **2008**, *14* (Suppl. S6), 2–8. [CrossRef]

30. Scarabelli, L.; Sánchez-Iglesias, A.; Pérez-Juste, J.; Liz-Marzán, L.M.A. "Tips and Tricks" Practical Guide to the Synthesis of Gold Nanorods. *J. Phys. Chem. Lett.* **2015**, *6*, 4270–4279. [CrossRef]
31. Suárez-López, R.; Puntes, V.F.; Bastús, N.G.; Hervés, C.; Jaime, C. Nucleation and growth of gold nanoparticles in the presence of different surfactants. A dissipative particle dynamics study. *Sci. Rep.* **2022**, *12*, 13926. [CrossRef]
32. Kumari, M.; Mishra, A.; Pandey, S.; Singh, S.P.; Chaudhry, V.; Mudiam, M.K.R.; Shukla, S.; Kakkar, P.; Nautiyal, C.S. Physico-Chemical Condition Optimization during Biosynthesis lead to development of Improved and Catalytically Efficient Gold Nano Particles. *Sci. Rep.* **2016**, *6*, 27575. [CrossRef] [PubMed]
33. Tufail, M.S.; Liaqat, I.; Andleeb, S.; Naseem, S.; Zafar, U.; Sadiqa, A.; Liaqat, I.; Ali, N.M.; Bibi, A.; Arshad, N.; et al. Biogenic Synthesis, Characterization and Antibacterial Properties of Silver Nanoparticles against Human Pathogens. *J. Oleo Sci.* **2022**, *71*, 257–265. [CrossRef]
34. Folorunso, A.; Akintelu, S.; Oyebamiji, A.K.; Ajayi, S.; Abiola, B.; Abdusalam, I.; Morakinyo, A. Biosynthesis, characterization and antimicrobial activity of gold nanoparticles from leaf extracts of *Annona muricata*. *J. Nanostructure Chem.* **2019**, *2*, 111–117. [CrossRef]
35. Ahmad, T.; Wani, I.A.; Manzoor, N.; Ahmed, J.; Asiri, A.M. Biosynthesis, structural characterization and antimicrobial activity of gold and silver nanoparticles. *Colloids Surf. B Biointerfaces* **2013**, *107*, 227–234. [CrossRef] [PubMed]
36. Burygin, G.L.; Khlebtsov, B.N.; Shantrokha, A.N.; Dykman, L.A.; Bogatyrev, V.A.; Khlebtsov, N.G. On the Enhanced Antibacterial Activity of Antibiotics Mixed with Gold Nanoparticles. *Nanoscale Res. Lett.* **2009**, *4*, 794–801. [CrossRef]
37. Grace, A.N.; Pandian, K. Antibacterial efficacy of aminoglycosidic antibiotics protected gold nanoparticles—A brief study. *Colloids Surf. A Physicochem. Eng. Asp.* **2007**, *297*, 63–70. [CrossRef]
38. Gu, H.; Ho, P.L.; Tong, E.; Wang, L.; Xu, B. Presenting Vancomycin on Nanoparticles to Enhance Antimicrobial Activities. *Nano Lett.* **2003**, *3*, 1261–1263. [CrossRef]
39. Tom, R.T.; Suryanarayanan, V.; Reddy, P.G.; Baskaran, S.; Pradeep, T. Ciprofloxacin-protected gold nanoparticles. *Langmuir* **2004**, *20*, 1909–1914. [CrossRef]
40. Saha, B.; Bhattacharya, J.; Mukherjee, A.; Ghosh, A.K.; Santra, C.R.; Dasgupta, A.K.; Karmakar, P. In vitro structural and functional evaluation of gold nanoparticles conjugated antibiotics. *Nanoscale Res. Lett.* **2007**, *2*, 614–622. [CrossRef]
41. Peacock, S.J.; Paterson, G.K. Mechanisms of Methicillin Resistance in *Staphylococcus aureus*. *Annu. Rev. Biochem.* **2015**, *84*, 577–601. [CrossRef] [PubMed]